
Article:
Jazany, R.A., Hajirasouliha, I., Moghadam, A.S. et al. (2 more authors) (2016) Analytical study on the seismic performance of steel braced frames with masonry infill. Journal of Structural Engineering, 142 (10). 04016083. ISSN 0733-9445

https://doi.org/10.1061/(ASCE)ST.1943-541X.0001548

ANALYTICAL STUDY ON THE SEISMIC PERFORMANCE OF STEEL BRACED FRAMES WITH MASONRY INFILL

Roohollah Ahmady Jazany [1], Iman Hajirasouliha [2], Abdolreza S Moghadam [3], Hossein Kayhani [4] and Hamidreza Farshchi [5]

Abstract

Special Concentrically Braced Frames (CBFs) are widely used as efficient lateral-load resisting systems in seismic regions. In this study, experimentally validated FE models are used to investigate the effects of masonry infill and gusset-plate configuration on the seismic performance of CBFs. It is shown that the presence of masonry infill can increase the initial stiffness and ultimate strength of CBFs by up to 35% and 52%, respectively. However, the frame-infill interaction imposes high plastic strain demands at the horizontal re-entrant corner of gusset plate connections, which may lead to premature failure of fillet welds under strong earthquakes. While using tapered gusset plates can significantly increase the fracture potential at fillet welds, gusset plates with elliptical clearance of eight times the plate thickness can lead to up to 54% lower equivalent plastic strain demands at both gusset plate connections and brace elements. While the effects of masonry infill are usually ignored in the seismic design process, the results highlight the importance of considering those effects in the seismic design of CBF elements and gusset plate connections.

Keyword: Concentrically Braced Frames, Masonry Infill, Gusset Plate, Fracture, Equivalent Plastic Strain

[1] Research Associate, Structural Engineering research Centre, International Institute of Earthquake Engineering and Seismology, Tehran, Iran. E-mail: r.ahmady@iiees.ac.ir

[2] Senior Lecturer (Associate Professor), Department of Civil and Structural Engineering, The University of Sheffield, Sheffield, UK. E-mail: i.hajirasouliha@sheffield.ac.uk

[3] Associate Professor, Structural Engineering research Centre, International Institute of Earthquake Engineering and Seismology, Tehran, Iran. E-mail: moghdam@iiees.ac.ir

[4] Assistant Professor, Department of Civil Engineering, Science and Research Branch, Islamic Azad University, Tehran, Iran. E-mail: h.kayhani@srbiau.ac.ir

[5] Research Associate, Structural Engineering research Centre, International Institute of Earthquake Engineering and Seismology, Tehran, Iran. E-mail: h.farshchi@iiees.ac.ir

Introduction

Special Concentrically Braced Frames (CBFs) are widely used as primary lateral-load resisting systems in seismic regions due to their ability in providing high lateral strength, stiffness and ductility (ANSI/AISC 341, 2010). While brace elements have a major role in controlling the inelastic lateral deformations of CBFs, gusset plate connections are designed to sustain large inelastic deformations after buckling of the braces (Thornton, 1991; Uriz and Mahin, 2004). Fracture of brace elements due to excessive post buckling deformations can result in poor seismic performance of CBFs (Yoo et al., 2007). Premature failure of gusset plate connections and fracture of fillet weld lines are also considered as unfavourable fracture modes in CBFs (Yoo et al. 2008).

Lehman et al. (2008) showed that the maximum strain demands of the beam and column elements of CBFs under earthquake loads may change significantly by changing the over strength characteristics of gusset plate connections. Hsiao et al. (2012) proposed a more accurate modelling approach to predict the seismic behaviour of CBFs by including the local behaviour of gusset plate connections as well as nonlinear geometric effects to simulate the buckling of brace elements. Roeder et al. (2006 and 2012) presented a new design method to balance the gusset plate yield mechanisms with the tensile yielding or buckling of the braces. In a follow up study, Lumpkin et al. (2012) conducted experimental tests on two three-storey CBFs with concrete slabs, and concluded that the balanced-design procedure results in thinner and more compact gusset plate connections and also a higher overall ductility in the CBFs.

CBFs with masonry infill represent a typical construction practice adopted in many developing countries such as Iran (see Fig. 1). The beam-column connections of these structures are usually simply supported or semi-rigid and, therefore, the seismic resistance is mainly provided by the frames with brace elements (Hashemi and Hassanzadeh, 2008). It is shown in Fig. 1 that the damages to CFBs with masonry infill during the 2003 Bam

earthquake were mainly due to the buckling of the braces, fracture of horizontal re-entrant corner of gusset plate connections and spalling of masonry infill. Several experimental programs have been conducted to investigate the actual seismic performance of steel frames with masonry infill under strong earthquake excitations (e.g. Mander et al., 1998; Moghaddam et al., 2006). These studies concluded that the presence of masonry infill improves the stability of the frame and the energy dissipation capacity of the system. However, observations from major devastating earthquakes (especially Bam earthquake in Iran) highlighted that ignoring the contribution of masonry infill in the seismic design process can lead to the premature fracture of the connections in CBFs.

The effect of brick infill walls on the seismic performance of eccentrically braced frames was studied by Daryan et al. (2009). By using an explicit finite element method, they demonstrated that the presence of masonry infill can increase the elastic range of the force-displacement behaviour, while the plastic deformation capacity of the frame will be deteriorated due to fragility of the masonry wall. However, the results of Daryan et al. (2009) study were based on the superposition of two distinct experimental tests on a CBF and a masonry infill wall and, therefore, could not capture the actual frame-infill interaction. In a more recent study, Ahmady Jazany et al. (2013) conducted a series of experimental tests to investigate the seismic performance of half-scale CBFs with masonry infill. They showed that the masonry infill can increase the lateral load-bearing capacity and the lateral stiffness of the frames by more than 40%. The results of their study also indicated that the presence of masonry infill may lead to premature fracture at the connection weld lines, which can significantly reduce the seismic performance and ductility of the CBFs.

To prevent or delay the premature failure modes in the connections of CBFs, the current study analytically investigates the seismic performance of CBFs with different gusset plate and weld configurations in the presence and the absence of masonry infill. Experimentally

validated FE models are used to obtain more efficient design solutions for practical applications in seismic regions.

Reference Experimental Programme

The cyclic lateral load tests on CBFs conducted by Ahmady Jazany et al. (2013) are used to validate detailed FE models in this study. The test specimens consisted of a concentrically braced steel frame without masonry infill (CBF) and a concentrically braced steel frame with masonry infill (CBFI), which were built at half-scale. Fig. 2 shows the test specimens CBF and CBFI and the experimental test setup. The distance between the centre-line of the columns and the height of the frame was 250 cm and 150 cm, respectively. The half-scale beam and column elements were fabricated using single IPE-270 and IPB-120 sections according to DIN-1025 (1995). Brace elements were UNP 60 with slenderness ratios λ_x= 56 and λ_y= 34. Infill panels consisted of half-scale solid clay bricks with the average size of 219 × 110 × 66 mm, which were placed in running bond with 22 courses.

The frame elements and gusset plate connections were designed based on ANSI/AISC 341-10 (2010). The corner and mid-height gusset plates were 280 × 280 × 8 mm and 250 × 250 × 12 mm, respectively. The beam-to-column connections were double seat angles. The gusset plate connections were designed with elliptical offset of 8tp (tp is the gusset plate thickness) to provide a balance between the yielding of the gusset plates and braces as suggested by Yoo et al. (2007 and 2008). The gusset plates were then welded to both brace and frame elements with 8 mm interface welds.

The CBFI specimen was designed to comply with the requirements of INBC-PART8 (2005). To evaluate the compressive strength of the masonry infill, 15 three-course block masonry prisms (couplet specimens) were tested based on ASTM C1314-14. The average prism compressive strength was 7.53 MPa that is less than the average compressive strength

of the brick and mortar. Based on common construction practice in Bam, a mortar with the similar characteristics to those applied for masonry infill was used to fill the gaps between the steel members and the masonry wall. The average thickness of the mortar was 8 mm and 5 mm next to the beam and column elements, respectively. To monitor cracking patterns, a very fine layer of low strength plaster was used on the masonry wall panel (less than 1 mm thickness). The effect of this low strength layer on the seismic performance of the CBFI was considered to be negligible. The experimental tests were displacement control under ATC 24 cyclic loads (see Fig. 3). More information about the reference tests can be found in Ahmady Jazany et al. (2013).

Failure Modes of the Reference Tests

Based on Ahmady Jazany et al. (2013) experimental results, the first yielding in the CBF test specimen occurred in the bracing elements at storey drift angle of 0.008 rad. The yielding started between the corner and mid-height gusset plates as shown in Fig 4(b), which was followed by diagonal yield lines on the gusset plates. Out-of-plane buckling of the braces started at storey drift angle of 0.012 rad and led to about 13.5 cm out-of-plane deformation at storey drift angle of 0.025 rad (see Fig 4(a)). The experimental test was stopped at this stage to prevent damage to laboratory equipment. As shown in Fig. 4(a) and (b), no fracture was observed at brace and gusset plate connections. Concurrence of flaking of the whitewashed areas on the brace elements (see Fig. 4 (a)) and the gusset plates (see Fig. 4 (c)) implies that the concept of balanced design was achieved in this test specimen. As shown in Fig. 4 (a) and 5(a) there was no sign of fracture on the gusset plate weld line up to the failure point.

Ahmady Jazany et al. (2013) observations showed that the infill-frame interaction in the CBFI specimen considerably increased the strain demands of column elements and gusset plate connections. The first yielding was observed in the steel columns at storey drift angle of

0.008 rad. The yielding of the gusset plate connections and brace elements started almost simultaneously at storey drift angle of 0.01 rad. At this stage, a significant part of the whitewashed masonry wall flaked off around the mid-height gusset plate connection. Subsequently, the brace elements exhibited out-of-plane buckling at drift angle of 0.012 rad, which was followed by the separation between the masonry infill and the braces as shown in Fig. 6(a) and (b). Stair-stepped cracks were then developed in the masonry infill followed by sliding cracks along the bed joints. This was concurrent with the fracture of the fillet weld at horizontal re-entrant corner of the gusset plate connection as shown in Fig. 5 (b), and the test was terminated at this stage. It should be noted that the damages observed in the CBFI test specimen (i.e. out-of-plane buckling of brace elements, cracking of masonry infill and the fracture of fillet weld at horizontal re-entrant corner of gusset plate connections) compare very well with the observations of the 2003 Bam earthquake in Iran (see Fig. 1).

The nonlinear hysteretic behaviour of the CBF and CBFI test specimens are compared in Fig. 7(a) and (b). While the peak and the ultimate load capacity of the CBF specimen was 282 kN and 258 kN, respectively, the corresponding values for the test specimen CBFI reached 398 kN and 405 kN. Based on the results shown in Fig. 7, the strength degradation of the CBF and CBFI specimens was 9% and 22% at failure, which occurred at drift angles of 0.025 and 0.015 rad, respectively. This implies that the presence of masonry infill not only reduced the deformation capacity of the special concentrically braced frame from 0.025 rad to 0.015 rad, but also considerably increased the strength degradation of the system.

In general, the similarity between the experimental results and the damage to typical CBFs with masonry infill in the 2003 Bam Earthquake in Iran (see Fig. 1) can demonstrate the adequacy of the selected half-scale models in this study.

Performance Parameters

Previous studies on fracture of metals under cyclic loading have shown that the von-Mises stress (or equivalent plastic stress) can be efficiently used to predict the yielding of steel material based on the results of simple uniaxial tensile tests (e.g. Yoo et al., 2008):

$$\sigma_{eqv} = \left(\frac{1}{2} \left[(\sigma_x - \sigma_y)^2 + (\sigma_y - \sigma_z)^2 + (\sigma_z - \sigma_y)^2 + 6(\sigma_{xy}{}^2 + \sigma_{xz}{}^2 + \sigma_{yz}{}^2) \right] \right)^{\frac{1}{2}} \quad (1)$$

where σ_x, σ_y, σ_z, σ_{xy}, σ_{yz} and σ_{zx} are components of the stress tensor.

Also the equivalent plastic strain (ε_{eqv}^{pl}) has been widely used to evaluate the strain demands and fracture potential of steel connections (El-Tawil et al. (1998); Kanvinde and Deierlein (2005); Yoo et al. (2007, 2008)). These studies suggested that the crack initiation can be adequately predicted by defining a threshold for ε_{eqv}^{pl}. For a given stress–strain state, ε_{eqv}^{pl} is calculated using the following equation:

$$\varepsilon_{eqv}^{pl} = \frac{1}{\sqrt{2}(1+\upsilon')} \left[\left(\varepsilon_x^{pl} - \varepsilon_y^{pl} \right)^2 + \left(\varepsilon_y^{pl} - \varepsilon_z^{pl} \right)^2 + \left(\varepsilon_z^{pl} - \varepsilon_z^{pl} \right)^2 + \frac{2}{3} \left(\gamma_{xy}^{pl^2} + \gamma_{yz}^{pl^2} + \gamma_{zx}^{pl^2} \right) \right]^{\frac{1}{2}} \quad (2)$$

where ε_x^{pl}, ε_y^{pl} and ε_z^{pl} are plastic strains, γ_{xy}^{pl}, γ_{yz}^{pl} and γ_{zx}^{pl} are plastic shear strains, and υ' is the effective Poisson's ratio. It should be noted that ε_{eqv}^{pl} may depend on the FE mesh size, crack location and stress conditions. Wang et al. (2011) study showed that using a threshold for ε_{eqv}^{pl} that is calibrated based on experimental results can be a reliable method to predict the crack initiation and propagation in welded connections.

Experimentally Validated FE Models

In this section, the nonlinear cyclic behaviour of CBFs with and without masonry infill is studied using detailed FE models validated with the reference experimental tests discussed in previous sections. The ANSYS (1998) finite element programme is used to perform inelastic

dynamic analyses. Fig. 8 shows the schematic view of the CBF and CBFI FE models and the critical points on the gusset plate connections. The steel elements and fillet welds were modelled using the 8-node 3D solid element SOLID45. The material properties were obtained from the measured stress–strain relationships reported by Ahmady Jazany et al. (2013). Contact elements (CONTA174) were used to simulate the contact and sliding between adjacent surfaces in the seat angle connections. Nonlinear buckling and large displacement analysis were conducted to model the buckling behaviour of the braces. The initial imperfections were taken into account by applying 0.000001 of the measured buckling displacements based on the dominant buckling mode shape of the brace elements as observed in the reference experimental tests.

The smeared crack element SOLID 65 was implemented to model the mortar and masonry unites. Based on the experimental results reported by Ahmady Jazany et al. (2013), the Young modulus (E) and the Poisson's ratio (υ) of the masonry unites were considered to be 2500 MPa and 0.25, respectively. The interaction between steel elements and masonry bricks was modelled using the contact pair elements CONTA174-TARGE170 with Coulomb friction coefficient (μ) of 0.45 as suggested by Shaikh (1978). The fracture of the masonry material was modelled using the Drucker–Prager yield criterion with no strengthening hardening. Pourazin and Eshghi (2009) showed that this pressure-dependent yield model is suitable for the modelling of masonry infill as it is capable of considering different tensile and compressive yield strength values. The William and Warnkle (1975) constitutive model was used to simulate cracking and crushing of masonry infill. The parameters used for the modelling of masonry infill are summarised in Table 1.

The cyclic loading protocol shown in Fig. 3 was applied to the CBF and CBFI FE models. Fig. 7 compares the hysteretic response obtained from the FE models of the test specimens CBF and CBFI and their corresponding experimental tests. Based on this figure, it is evident

that the FE models could accurately predict the non-linear load-displacement behaviour of the specimens with less than 10% error.

The von-Mises stress distribution results for the CBF and CBFI specimens are displayed in Figs. 4 and 6, respectively. The results show a good agreement between the maximum von-Mises stress at the critical points of the gusset plate connections and the fracture of fillet welds at horizontal re-entrant corner of the gusset plates in the reference experimental tests (see Fig. 5). Based on Fig. 4(c) and (f), the von-Mises stress distribution in the gusset plate connections is also match with the flaking of the whitewashed area on the gusset plates.

It is shown in Fig. 4(a) and (d) that the developed FE model could simulate the out-of-plane buckling behaviour of the brace elements of the CBF specimen similar to the test observations. It is also shown that the von-Mises stress distributions obtained from the FE model, in general, compare well with the yielding locations of the braces, recognised by the flaking of the whitewashed areas.

The comparison between the von-Mises stress distribution and the experimental results in Fig. 6 shows that the FE model of the infill panel could identify the crushing zones in the CBFI specimen. The out-of-plane buckling of the brace elements predicted by the FE models in Fig. 6(d) is in good agreement with the experimental observations in Fig. 6(b). The brace elements of the CBFI specimen exhibited about 5.2 cm out-of-plane buckling at the end of the experimental test, which is in good agreement with 4.7 cm out-of-plane displacement predicted from the FE model.

The above comparisons indicate that the detailed FE models could simulate the buckling mode of the braces, fracture of the gusset plate connections, and the crushing of the masonry infill panel with an acceptable accuracy as was observed in the reference experimental tests and actual damages to CBFs in the 2003 Bam earthquake.

Effects of Gusset Plate Configuration on the Performance of CBFs

As discussed in the previous sections, the dominant failure mode of the test specimen with masonry infill (CBFI) was the fracture of fillet welds in the re-entrant corners of gusset plate connections. In this study, the experimentally validated FE models introduced in the previous section are used to examine the effects of different gusset plate configurations on the seismic performance of CBFs.

Companion Analytical Models

Four groups of CBFs were designed according to AISC (2010) by using straight and tapered gusset plates with linear and elliptical clearance (see Table 2). Similar to the common practice, the frames were designed by ignoring the effects of infill-frame interactions. Fig. 9 demonstrates the configuration of the gusset plate connections of the designed CBFs with and without masonry infill.

The first configuration of the gusset plate was based on elliptical clearance of $8t_p$ (t_p is gusset plate thickness), which was used in the reference experimental tests (Ahmady Jazany et al., 2013). As mentioned before, this gusset plate configuration is recommended by Yoo. et al. (2007, 2008) to have a balanced failure in brace elements and gusset plate connections. The second gusset plate configuration had a $2t_p$ linear clearance based on AISC seismic provisions (2010). The third and the fourth configurations were tapered gusset plates with inclination angle of $15°$ and $25°$, respectively. These two gusset plate configurations are used in engineering practice and their performance has been investigated by Yoo et al. (2007, 2008).

Using the above-mentioned gusset plate configurations, a total of eight FE models were developed to simulate the non-linear seismic behaviour of CBFs with the presence and the absence of masonry infill. A summary of the FE models including gusset plates' geometry, frame elements and the angle and the length of the brace elements welded on the gusset plates are presented in Table 2.

The rupture potential of different gusset plate connections

The premature fracture of gusset plate weld lines in CBFs is an unfavourable failure mode (Farshchi and Moghadam, 2004; Yoo et al., 2008; Ahmady Jazany et al., 2013), which can considerably affect the seismic performance of the whole structural system under strong earthquakes. To evaluate the rupture potential of gusset plate connections, equivalent plastic strains (ε_{eqv}^{pl}) are calculated at the critical points of the gusset plate connections. The critical points (points a, b, c and d in Fig. 8) are identified based on the experimental test observations and also high stress demand regions in FE models. As discussed before, higher equivalent plastic strain (ε_{eqv}^{pl}) values are usually associated with an increased risk of crack initiation and fracture.

Fig. 10 compares the equivalent plastic strain (ε_{eqv}^{pl}) distribution of gusset plate connections with different configurations in the CBFs with and without masonry infill at storey drift angle of 0.025 rad. The results indicate that the maximum ε_{eqv}^{pl} values on the horizontal re-entrant corner of the gusset plates in the frames with masonry infill (i.e. CBFI-a, CBFI-b and CBFI-c) are approximately 3 times higher than the corresponding values in the similar bare frames (i.e. CBF-a, CBF-b and CBF-c). The results also show that the distribution of ε_{eqv}^{pl} in the re-entrant corners of the gusset plates is more uniform in the models without masonry infill. Based on Fig. 10, using an elliptical clearance gusset plate configuration (i.e. CBFI-a and CBF-a models) leads to considerably lower maximum equivalent plastic strains (up to 54% less) compared to other gusset plate configurations. It is also shown that, both in the presence and the absence of masonry infill, the gusset plates with tapered configuration exhibited maximum equivalent plastic strains. This implies that using tapered gusset plates, in general, will increase the potential of premature failure in the connections.

Optimum gusset plate configurations

To investigate the effects of using different gusset plate configurations on the plastic strain demands of the CBFs connections, Fig. 11 compares the equivalent plastic strain (ε_{eqv}^{pl}) at the critical points of the gusset plates (points a, b, c, and d in Fig. 8) at different storey drift angles. As it was expected, for the same storey drift angle, the equivalent plastic strains in the gusset plate connections of the CBFs with masonry infill were significantly higher (up to three times more) compared to those without masonry infill. The presence of masonry infill also changed the most critical points of the gusset plate connections. It is shown in Fig. 11 that the points c and d on the gusset-plates (see Fig. 8) exhibited maximum fracture positional in CBFI (with masonry infill) and CBF (without masonry infill) models, respectively. This observation is consistent with the equivalent plastic strain distributions shown in Fig. 10.

Based on the results of the reference experimental tests, the threshold for ε_{eqv}^{pl} to initiate cracking in gusset plate connections was calculated to be in the range of 0.028 (lower bond) to 0.032 (upper bond). It is shown in Fig. 11(a) that the gusset-plate connections of the CBFI-a model (CBFI test specimen in Fig. 2) reached the crack initiation threshold at storey drift angle of around 0.015 rad, which compares very well with the experimental results presented in Fig. 7(b) and Fig. 5(b). The maximum ε_{eqv}^{pl} at the critical points of the gusset plate connections in CBF-a model (CBF test specimen in Fig. 2) was less than the cracking threshold up to the storey drift angle of 0.025 rad, where the test was stopped. This implies that no cracking at the horizontal re-entrant corner of the gusset plates was expected at the end of the cyclic tests, which is confirmed by the experimental test observations (see Fig. 5 (a)).

According to AISC 341 (2010) seismic provision, gusset plate connections in CBFs should be able to sustain an inter-storey drift angle of at least 0.025 rad, if they are connected to both beam and column elements. It is shown in Fig. 11 that the maximum equivalent plastic strains

(ε_{eqv}^{pl}) at the critical points of all CBFs with masonry infill clearly exceeded the crack initiation threshold at storey drift angle of 0.025 rad, due to the extra demand induced by the frame-infill interaction. For example, it is shown in Fig. 11(b) that the maximum ε_{eqv}^{pl} in the gusset plate connections of the CBF model, designed based on AISC 341 (2010) seismic provision, was less than the crack initiation threshold up to the storey drift angle of 0.025 rad. However, in the presence of masonry infill, the maximum equivalent plastic strains in the gusset plate connections exceeded the calculated crack initiation threshold at storey drift angle of around 0.015 rad. This means that this CBF cannot sustain the AISC required inter-storey drift angle, and hence is not qualified for seismic applications. These results can explain the extensive damage to CBFs with masonry infill in the 2003 Bam earthquake in Iran (Farshchi and Moghadam, 2004).

Figs 11(c) and 11(d) show that, in general, using tapered gusset plate configurations increased the equivalent plastic strains (ε_{eqv}^{pl}) at the critical points of the gusset plate connections. For example, it is shown that the tapered gusset plate with taper angle of 25° (configuration type d) exhibited up to 30% higher ε_{eqv}^{pl} compared to the gusset plate with elliptical clearance (configuration type a). Even in the frames without masonry infill, the maximum ε_{eqv}^{pl} at the gusset plate connections with tapered configuration was around 50% higher than the cracking initiation threshold at storey drift angle of 0.025 rad. Therefore, this type of gusset plate connection is not considered to be qualified based on AISC seismic provisions (2010).

For a better comparison, Table 3 presents the maximum ε_{eqv}^{pl} at the critical points of the gusset plate connections and brace elements of the eight CBFs shown in Fig. 9. The ultimate storey drift angle was considered to be 0.015 and 0.025 rad for the models with and without

masonry infill, respectively, based on the ultimate storey drift angles observed in the reference experimental tests as discussed in the previous sections.

It is shown in Table 3 that in the CBFs without masonry infill, the brace elements exhibited significantly higher equivalent plastic strains (ε_{eqv}^{pl}) compared to the gusset plate connections. Therefore, the failure of the CBFs without masonry infill was always due to the buckling of the brace elements, as it was also observed in the reference experimental tests. However, in the presence of masonry infill, the most critical locations with maximum ε_{eqv}^{pl} were on the gusset plates. This implies that gusset plate connections played a more dominant role in the failure of CBFs with masonry infill. Therefore, ignoring the effects of masonry infill in the seismic design of CBFs may reduce the deformability of the structural system and lead to a premature failure of the connections under strong earthquakes.

The results in Table 3 indicate that using the balance design concept (i.e. gusset plate configuration type a) will lead to lower equivalent plastic strain demands at both gusset plate connections and brace elements. While tapered gusset plate configurations are widely used in engineering practice (especially in developing countries), it is shown in Table 3 that using tapered gusset plates (i.e. c and d configurations) will considerably increase the maximum ε_{eqv}^{pl} at both gusset plates and brace elements. This is more evident for CBFs with masonry infill, in which tapered plates can result in two times higher plastic strains at the gusset plate connections compared to other configurations.

To study the effects of gusset plate configurations on the non-linear seismic behaviour of CBFs with and without masonry infill, Fig. 12 compares the envelope of the cyclic response (i.e. back bone curve) of the eight CBF and CBFI analytical models with different gusset plate configurations. Table 4 summarizes the mechanical properties of the models including yielding force, ultimate strength and initial stiffness based on idealized bi-linear back bone curves according to FEMA 356. It is shown that, in the absence of masonry infill, the

configuration of the gusset plates could affect the stiffness and the ultimate strength of the CBFs by up to 15% and 10%, respectively. However, as it was expected, the effect of gusset plate configuration on the strength and stiffness of CBFs with masonry infill was negligible (less than 4%). Table 4 also shows that, in general, using tapered gusset plates leads to a lower lateral stiffness and strength compared to other gusset plate configurations.

The results in Fig. 12 and Table 4 indicate that the presence of masonry infill, on average, increased the yielding force, ultimate strength and initial stiffness of the CBFs by 71%, 44% and 27%, respectively. However, the CBFs with masonry infill show negative stiffness after the yield point (softening behaviour) and also significantly lower displacement ductility levels under cyclic loads. This can be attributed to the premature fracture of the gusset plate welds as discussed in the previous sections. Also it can be noted from Fig. 12 that the envelope of the cyclic response of CBFs with masonry infill exhibits a descending branch only in one direction. This behaviour is due to the interaction between the masonry infill and the brace elements and is in agreement with the experimental observations (see Fig. 7). After buckling of a brace element in one direction, the presence of masonry infill prevents the return of the element to its initial state in the other direction. This leads to an asymmetric cyclic behaviour in CBFs with masonry infill.

To investigate the effect of using multi-wythe masonry walls on the seismic performance of CBFs, the maximum equivalent plastic strains (ε_{eqv}^{pl}) at the critical points of the gusset plate connections are calculated for the frames with double and triple wythe masonry walls as shown in Fig. 13. The results indicate that, compared to CBFs with single wythe masonry walls, using double-wythe and triple-wyrhe walls increased the maximum equivalent plastic strains at the gusset plate connections by up to 13% and 32%, respectively. This can considerably increase the likelihood of fillet weld fracture and premature failure of gusset plate connections under strong earthquakes.

Summary and Conclusions

Detailed FE models, validated by an experimental joint study, were used to study the effects of masonry infill and configuration of gusset plate connections on the seismic performance and failure modes of Concentrically Braced Frames (CBFs). Four groups of CBFs were designed by using straight gusset plates (with linear and elliptical clearance) and tapered gusset plates. It was shown that the developed FE models could predict the non-linear cyclic behaviour, damage development and failure patterns of CBFs with and without masonry infill similar to the reference experimental tests. Based on the results of this study, the following conclusions can be drawn:

- While using masonry infill panels in CBFs can reduce the maximum strain demands at braces, the interaction between masonry infill and steel frame may significantly increase (by up to 300%) the maximum equivalent plastic strains at the horizontal re-entrant corner of gusset plate connections. Therefore, the failure of CBFs with masonry infill is usually due to the premature fracture of gusset plate weld lines as was observed in the reference experimental tests and the 2003 Bam Earthquake in Iran.
- In the presence of masonry infill, the gusset plates designed by ignoring the effects of frame-infill interaction exceeded the crack initiation threshold at storey drift angle of around 0.015 rad, which implies these connections do not meet the ANSI/AISC 341-10 (2010) minimum requirements for seismic regions (i.e. storey drift angle of 0.025 rad). This can explain the extensive damage to CBFs with masonry infill in the Bam Earthquake.
- Gusset plate connections have a major role in controlling the inelastic behaviour of CBFs. Using gusset plates with elliptical clearance of 8tp (i.e. balance design) will lead to lower equivalent plastic strain demands (by up to 54%) at both gusset plate connections and brace elements. In contrast, using tapered gusset plate configurations can significantly

increase the plastic strain demands and fracture potential at gusset plate connections, both in the absence and the presence of masonry infill.

- While the configuration of gusset plates can change the initial stiffness and the ultimate strength of CBFs without masonry infill by up to 15%, the effect of gusset plate configuration on the mechanical properties of CBFs with masonry infill is negligible.
- The presence of masonry infill can increase the yielding force, ultimate strength and initial stiffness of CBFs by up to 80%, 52% and 35%, respectively. However, CBFs with masonry infill exhibit significantly lower ductility and post-yield stiffness compared to similar frames without masonry infill.
- Using multi-wythe masonry walls can considerably increase the fracture potential at the fillet welds of gusset plate connections under strong earthquakes. It was shown that CBFs with double-wythe and triple-wyrhe masonry walls exhibit up to 13% and 32% higher equivalent plastic strains at the gusset plate connections, respectively, compared to a similar frame with single-wythe wall.

The outcomes of this study in general highlight the importance of considering the effects of infill-frame interactions in the design process of CBFs and gusset plate connections in seismic regions. The presented results can be directly used for more efficient design of CBFs using conventional displacement-based or force-based design methods.

Acknowledgements

The authors would like to thank the Director of Structural Research Centre and all technicians and technical staff at IIEES for their valuable assistance.

References

Ahmady Jazany, R., Hajirasouliha, I. and Farshchi, H. (2013). "Influence of masonry infill on the seismic performance of concentrically braced frames", J. Constr. Steel. Res., 88, 150–163.

AISC. (American Institute of Steel Construction). (2001). "Manual of steel construction load and resistance factor design." 3rd ed. Chicago (IL).

ANSI/AISC 341–10. (2010). "Seismic provisions for structural steel buildings." Chicago (IL): American Institute of Steel Construction.

ANSYS. (1998). "User's Manual." Version 5.4, 201. Johnson Road., Houston, ANSYS Inc.

ASTM C1314-14. (2014). "Standard Test Method for Compressive Strength of Masonry Prisms", ASTM International, West Conshohocken (PA).

ATC 24. (1992). "Guidelines for cyclic seismic testing of components of steel structures." Applied Technology Council.

Daryan, A.S., Ziaei, M., Golafshar, A., Pirmoz, A. and Assareh M.A. (2009). "A study of the effect of infilled brick walls on behavior of eccentrically braced frames using explicit finite elements method." Am. J. Eng. Appl. Sci., 2(1), 96–104.

DIN 1025. (1995). "Hot rolled I and H sections: dimensions, mass and static parameters." Berlin, DIN, Deutsches Institut Fur Normung, EV.

El-Tawil, S., Mikesell T., Vidarsson E. and Kunnath. S.K. (1998). "Strength and ductility of FR welded-bolted connections." Report No. SAC/BD-98/01, SAC Joint Venture, Sacramento, California.

Farshchi, HR. and Moghadam, AS., (2004). "Damage of steel structures in Bam earthquake." Report No. BAM 213. Iran, International Institute of Earthquake Engineering and Seismology (IIEES).

FEMA 356. (2000) “Prestandard and commentary for the seismic rehabilitation of buildings.” Federal Emergency Management Agency.

Hashemi, B.H. and Hassanzadeh, M. (2008). “Study of a semi-rigid steel braced building damaged in the Bam earthquake.” J Constr. Steel Res., 64, 704–21.

Hsiao, P.C., Lehman D.E. and Roeder, C.W. (2012) .“Improved analytical model for special concentrically braced frames .” J. Constr. Steel Res., 73, 80-94.

INBC-Part 8. (2005). “Design and construction of masonry buildings.” Iranian national building code, Part 8, Ministry of Housing and Urban Development, Iran.

Kanvinde, A.M., Deierlein, G.G. (2005). “Continuum based micro models for ultra low cycle fatigue crack initiation in steel structures.” Proceeding, Structures Congress and Exposition, ASCE, Reston Va.

Lehman D.E., Roeder C.W., Herman D., Johnson S. and Kotulka B. (2008). “Improved seismic performance of gusset plate connections.” J. Struct. Eng. ASCE, 134,6,890–901.

Lumpkin, E.J., Hsiao, P., Roeder, C.W., Lehman, D.E., Tsai, C., Wu A., Wei, C. and Tsai, K., (2012) “Investigation of the seismic response of three-story special concentrically braced” J. Constr. Steel. Res.,77, 131-144.

Mander, J.B., Nair, B., Wojthowski, K and Ma J. (1998). “An experimental study on the seismic performance of brick-infilled steel frames with and without retrofit.” Technical report, NCEER 93–0001.

Moghadam, H.A., Mohammadi, M.Gh., Ghaemian, M. (2006). “Experimental and analytical investigation into crack strength determination of infilled steel frames.” J Constr Steel Res; 62,1341–52.

Pourazin, K. and Eshghi, S. (2009). “In-plane behaviour of a confined masonry wall.” TMS J, 27(1), 21–34.

Roeder C.W., Lehman, D.E and Yoo J.H. (2006). “Improved design of steel frame connections.” Int. J. Steel Struct, 5(2), 141–53.

Roeder, C.W., Lumpkin, E.J. , Lehman, D.E. (2012) “A balanced design procedure for special concentrically braced frame connections.” J. Constr. Steel Res. 73, 80–94.

Shaikh, AF. (1978). “Proposed revisions to shear-friction provisions.” PCI J, 23(2),12–21.

Thornton, WA. (1991). “On the analysis and design of bracing connections.” Proceedings of National Steel Construction Conference. Chicago (IL), AISC,1–33 [Section 26].

Uriz, P., Mahin S. (2004).“Seismic performance of concentrically braced steel frame buildings.” Proceedings, 13th world congress on earthquake engineering, Paper ID 1639.

Wang, Y., Zhou, H., Shi, Y. and Xiong, J. (2011). “Fracture prediction of welded steel connections using traditional fracture mechanics and calibrated micromechanics based models.” Int. J. Steel Struct., 11(3), 351-366.

William, K.J. and Warnkle, E.D. (1975). “Constitutive model for the triaxial behavior of concrete.” Proceedings of the International Assignment for Bridge and Structural Engineering, 19,174–86.

Yoo, J.H., Lehman, D.E. and Roeder, C.W. (2008).“Influence of connection design parameters on the seismic performance of braced frames.” J. Constr. Steel Res., 64,607–23.

Yoo J.H., Roeder C.W. and Lehman D. (2007).“Analytical performance simulation of special concentrically braced frames simulation and failure analysis of special concentrically braced frame tests.” J. Struct. Eng. (ASCE), 134(6), 881–9.

Table 1. Parameters used in the modelling of masonry material

Drucker-Prager yield criterion		**William and Wrankle model**	
c	$0.88\,kg/cm^2$	f_c	$40\,kg/cm^2$
η	15°	f_t	$1\,kg/cm^2$
φ	38°	β_t	0.75
		β_c	0.15

Table 2: Member sizes and gusset plate configurations of the FE models

Category	**Model**		**Assigned Clearance**	**Gusset Plate (mm)**	**Gusset plate thickness t_p (mm)**	**Frame Elements***	**Brace Angle and Brace Length on Gusset Plate (mm)**
	Without Infill	**With Infill**					
Elliptical Clearance	CBF-a	CBFI-a	$8t_p$	280×280	8	IPE270 IPB120 UNP60	37° 216
Linear Clearance	CBF-b	CBFI-b	Linear $2t_p$	320×320	8		37° 210
Tapered-T15	CBF-c	CBFI-c	$8t_p$	Taper of 15° 350×350	8		37° 286
Tapered-T25	CBF-d	CBFI-d	$8t_p$	Taper of 25° 410×410	10		37° 330

* IPE, IPB and UNP sections are used for beam, column and brace elements, respectively.

Table 3: Maximum equivalent plastic strains (ε_{eqv}^{pl}) at gusset plates and brace elements in the concentrically braced frames with and without masonry infill

Concentrically braced frames without masonry infill	Maximum ε_{eqv}^{pl} at storey drift angle 0.025 rad		Concentrically braced frames with masonry infill	Maximum ε_{eqv}^{pl} at storey drift angle 0.015 rad	
	Gusset Plates	Braces		Gusset plates	Braces
CBF-a	0.015	0.88	CBFI-a	0.032	0.038
CBF-b	0.029	0.95	CBFI-b	0.043	0.037
CBF-c	0.044	0.99	CBFI-c	0.052	0.040
CBF-d	0.049	1.12	CBFI-d	0.065	0.043

Table 4: Mechanical properties of the CBFs with different gusset plate configurations

Mechanical Properties of the Analytical Models	Elliptical Clearance		Linear Clearance		Tapered T15		Tapered T25	
	CBF-a	CBFI-a	CBF-b	CBFI-b	CBF-c	CBFI-c	CBF-d	CBFI-d
Yielding Force (KN)	195	315	178	320	190	323	185	319
Ultimate Strength (KN)	270	376	282	385	256	388	260	382
Stiffness (KN/m)	26270	30208	25320	31230	23810	31524	22950	31051

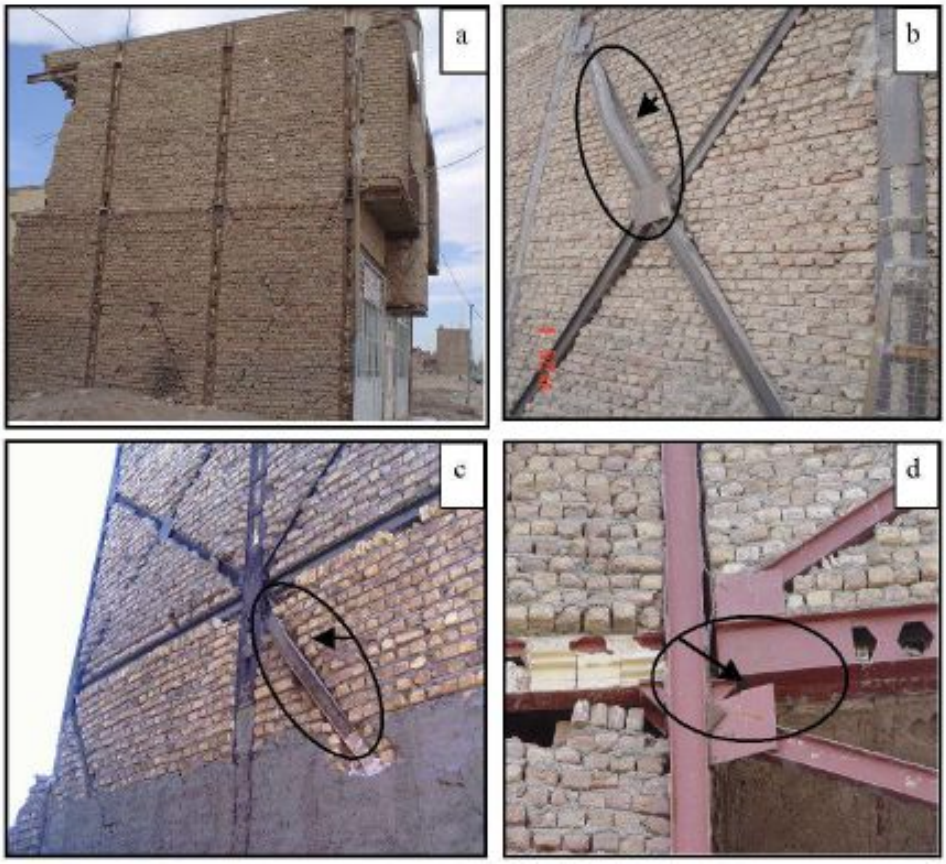

Fig. 1: (a) A typical CBF with masonry infill in Bam, Iran; (b, c) Buckling of X braces and (d) Fracture of horizontal re-entrant corner of gusset plate weld line and spalling of masonry infill in the 2003 Bam earthquake

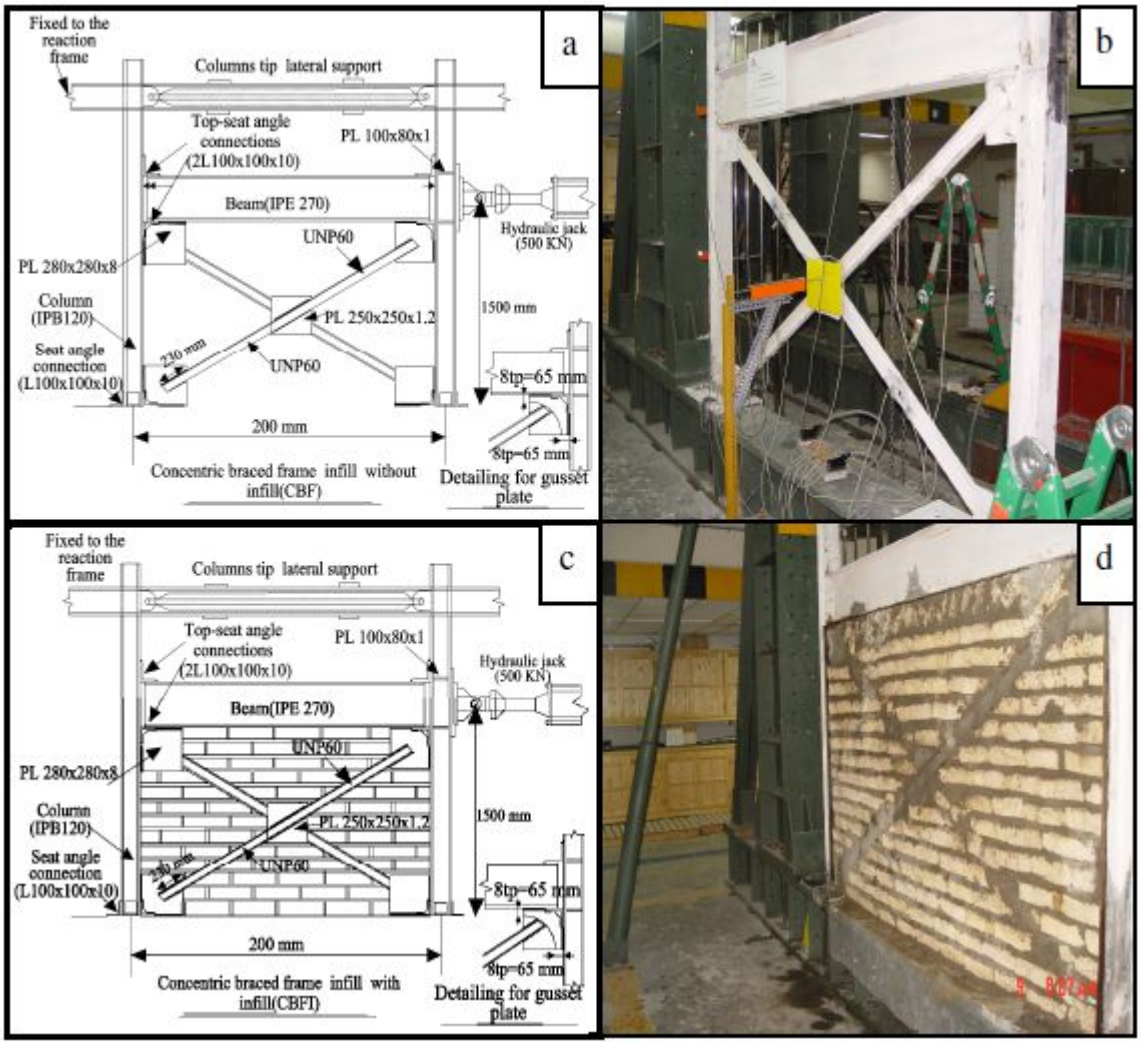

Fig. 2: Schematic and side view of the reference test specimens in Ahmady Jazany et al. (2013) study

(a, b) CBF specimen; (c, d) CBFI specimen

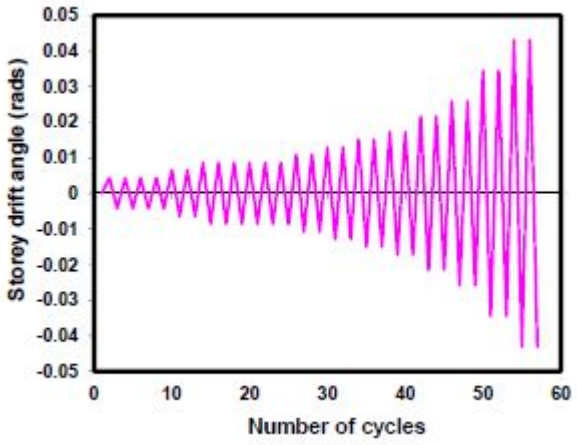

Fig. 3: Applied loading pattern (ATC 24)

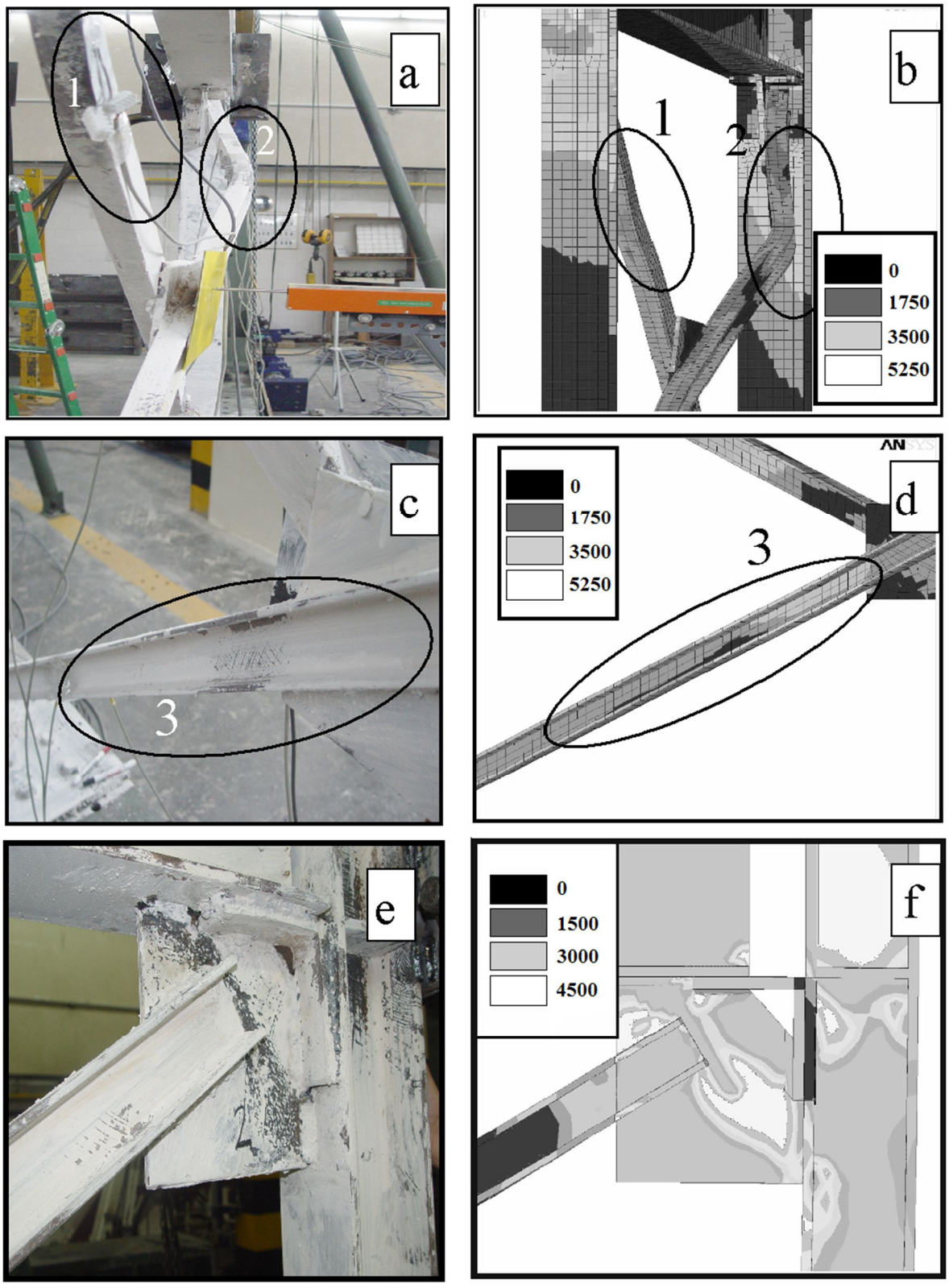

Fig. 4: Comparison between experimental observations and FE results for CBF (a) Out-of-plane buckling of braces; (b) Whitewashed area on brace element; (c) Whitewashed area on gusset plate connection; (d, e, f) von-Mises stress distributions in the corresponding FE model

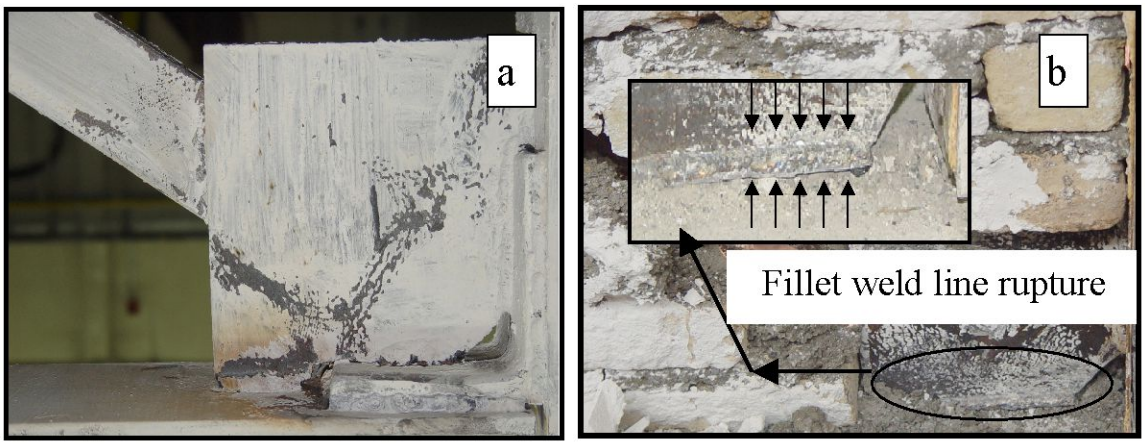

Fig. 5: (a) Yield lines on the gusset plate connection of CBF; (b) Fracture of fillet weld at horizontal re-entrant corner of the gusset plate connection of CBFI

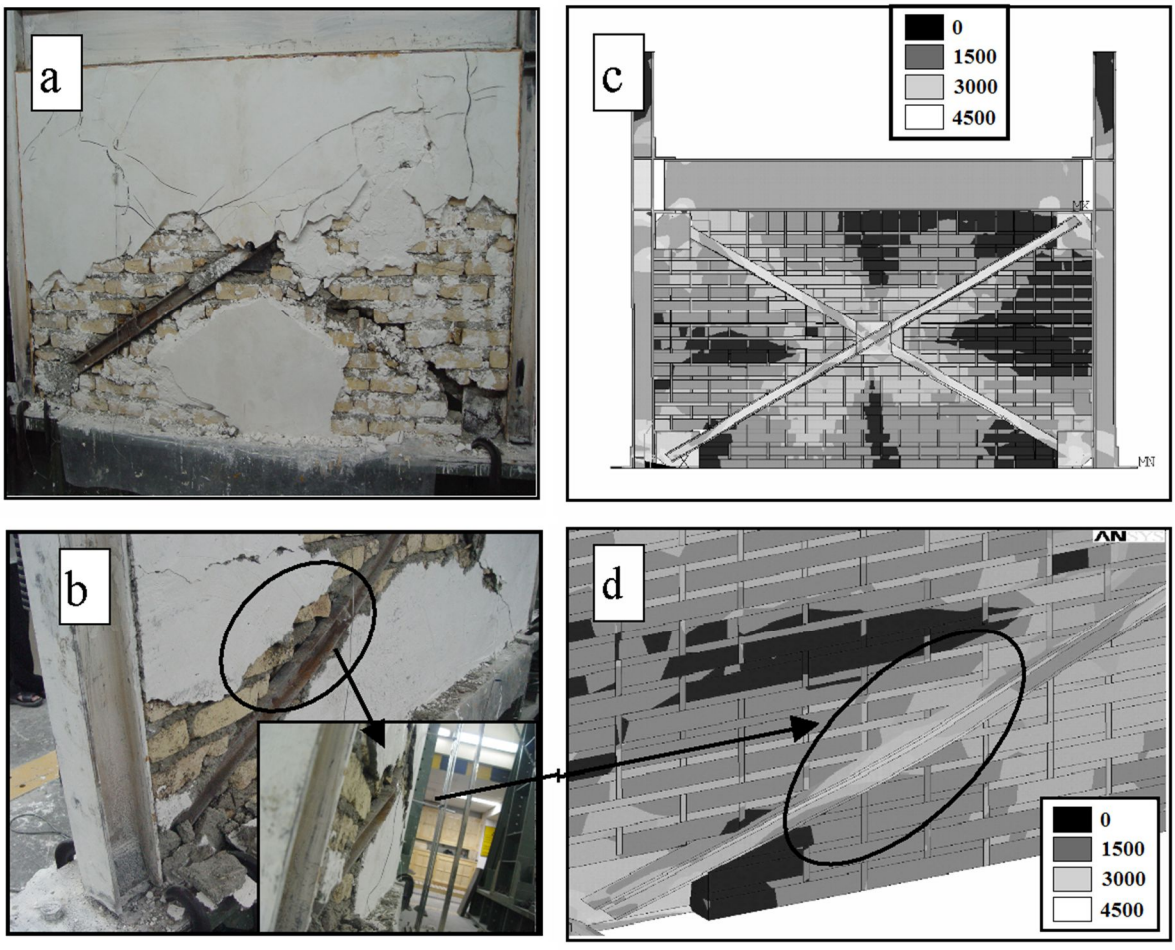

Fig. 6: (a, b) Out-of-plane buckling of brace elements in CBFI at storey drift angle of 0.015 rad; (c, d) von-Mises stress distribution in the corresponding FE model

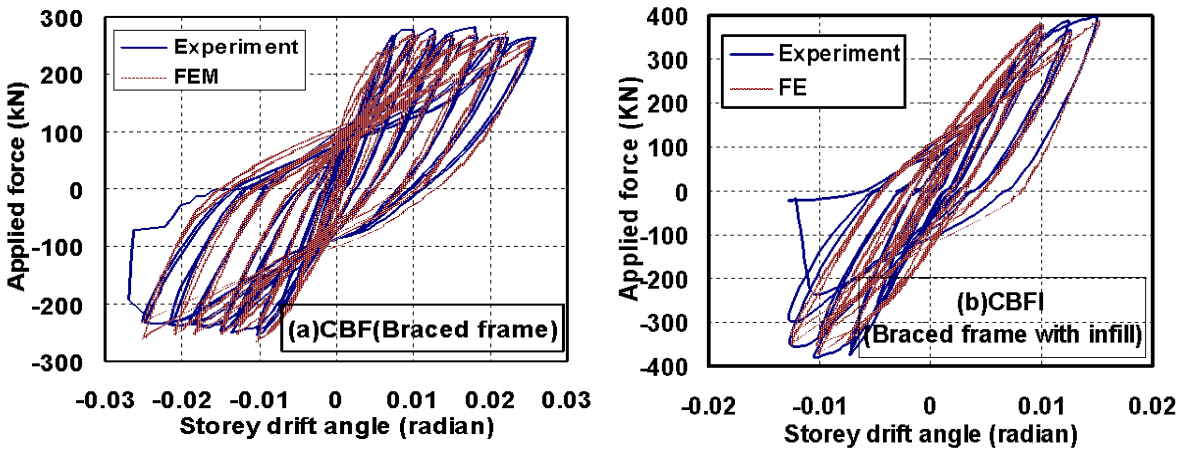

Fig. 7: Experimental and analytical load–displacement response of test specimens (a) CBF (b) CBFI

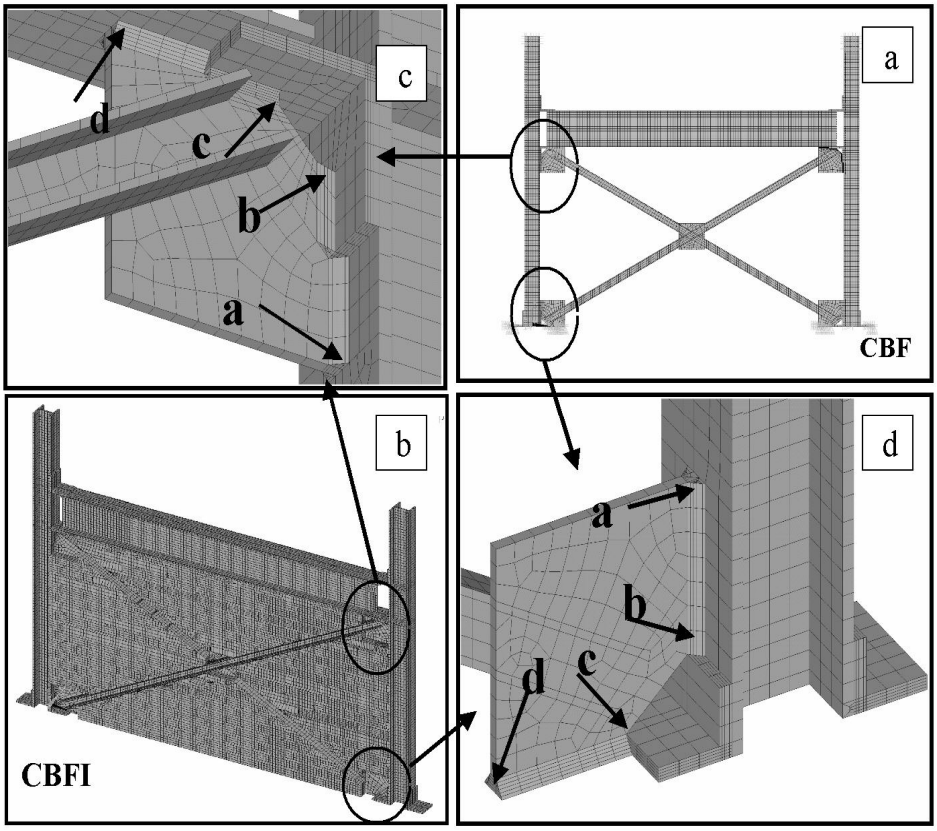

Fig. 8: FE models of test specimen (a) CBF; (b) CBFI; (c) Critical points on top gusset plate connection; (d) Critical points on bottom gusset plate connection

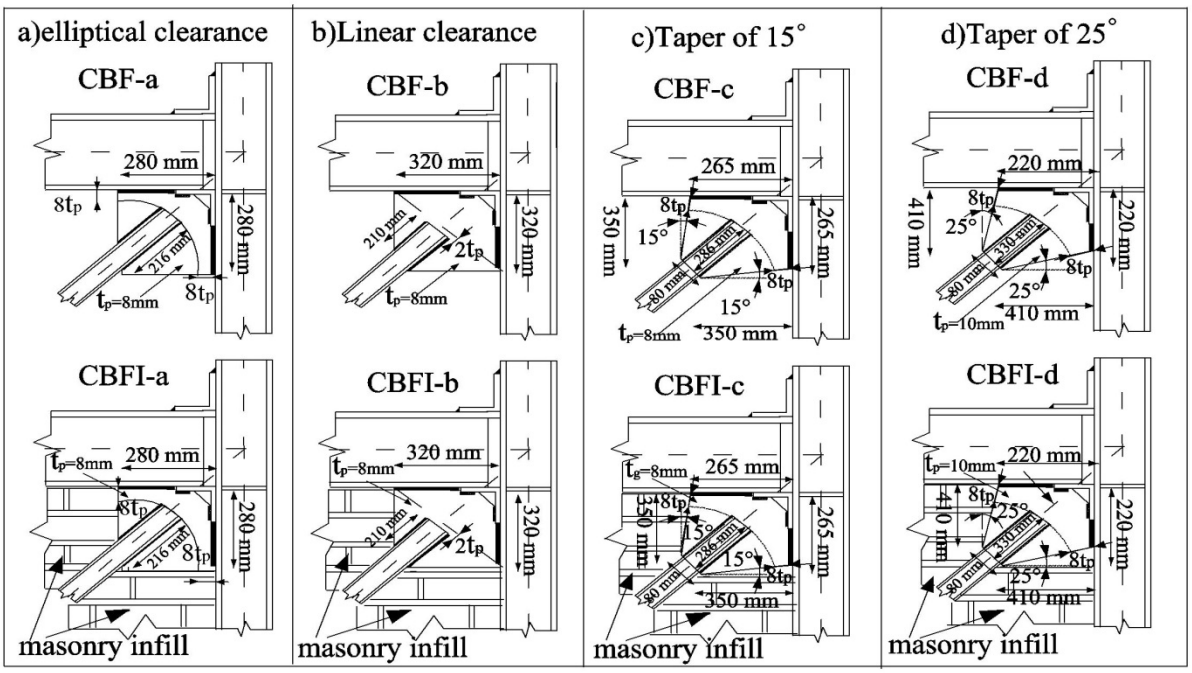

Fig. 9: Gusset plate connection configurations (a) Elliptical clearance 8tp; (b) Linear clearance 2tp; (c) Tapered gusset plate with inclination angle 15 and elliptical clearance 8tp; (d) Tapered gusset plate with inclination angle 25 and elliptical clearance 8tp

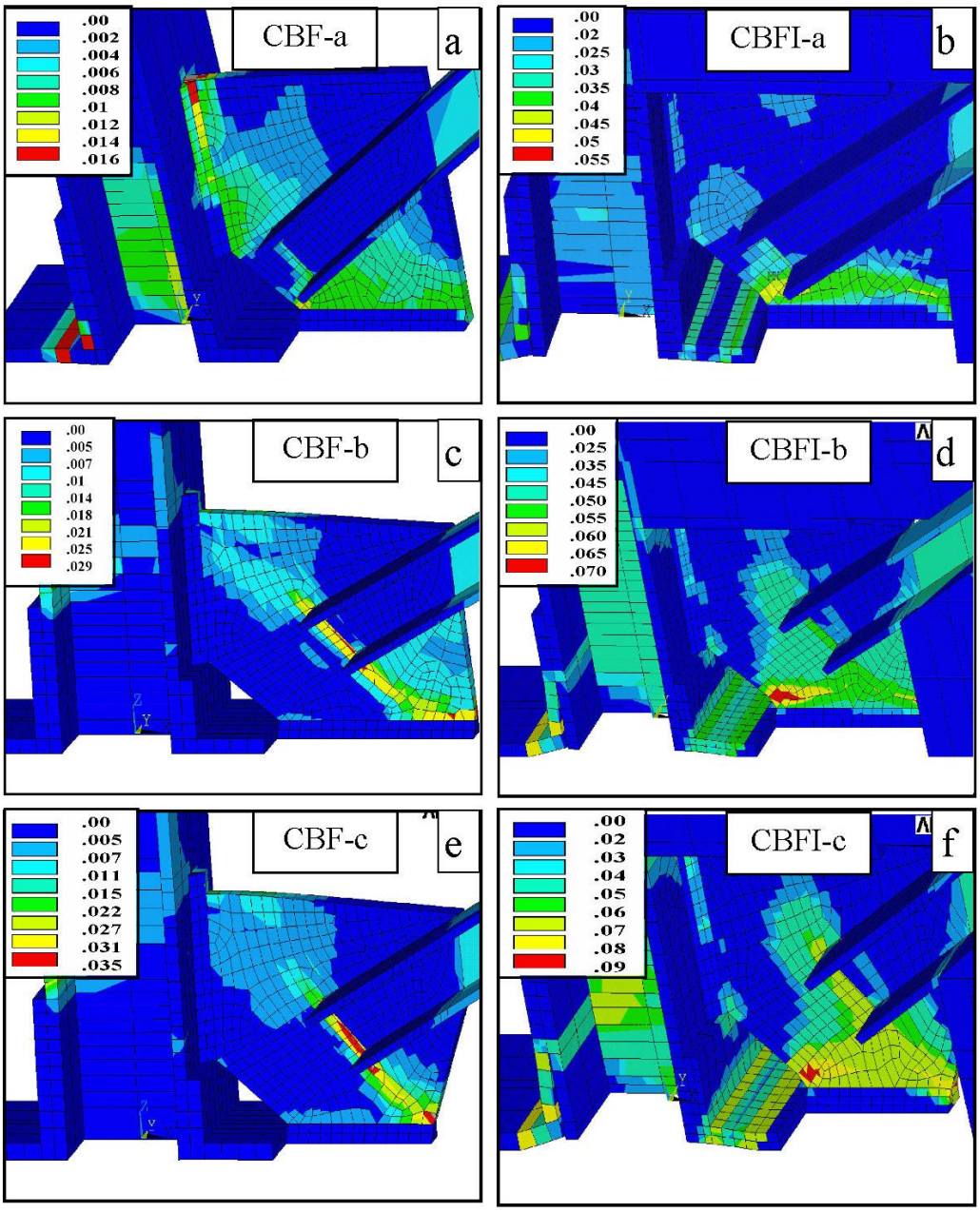

Fig. 10: Equivalent plastic strain (ε_{eqv}^{pl}) distribution of gusset plate connections in the frames with and without masonry infill at storey drift angle of 0.025 rad (a, b) Elliptical clearance 8tp; (c, d) Linear clearance 2tp; (e, f) Tapered gusset plate with taper angle of 15 degrees

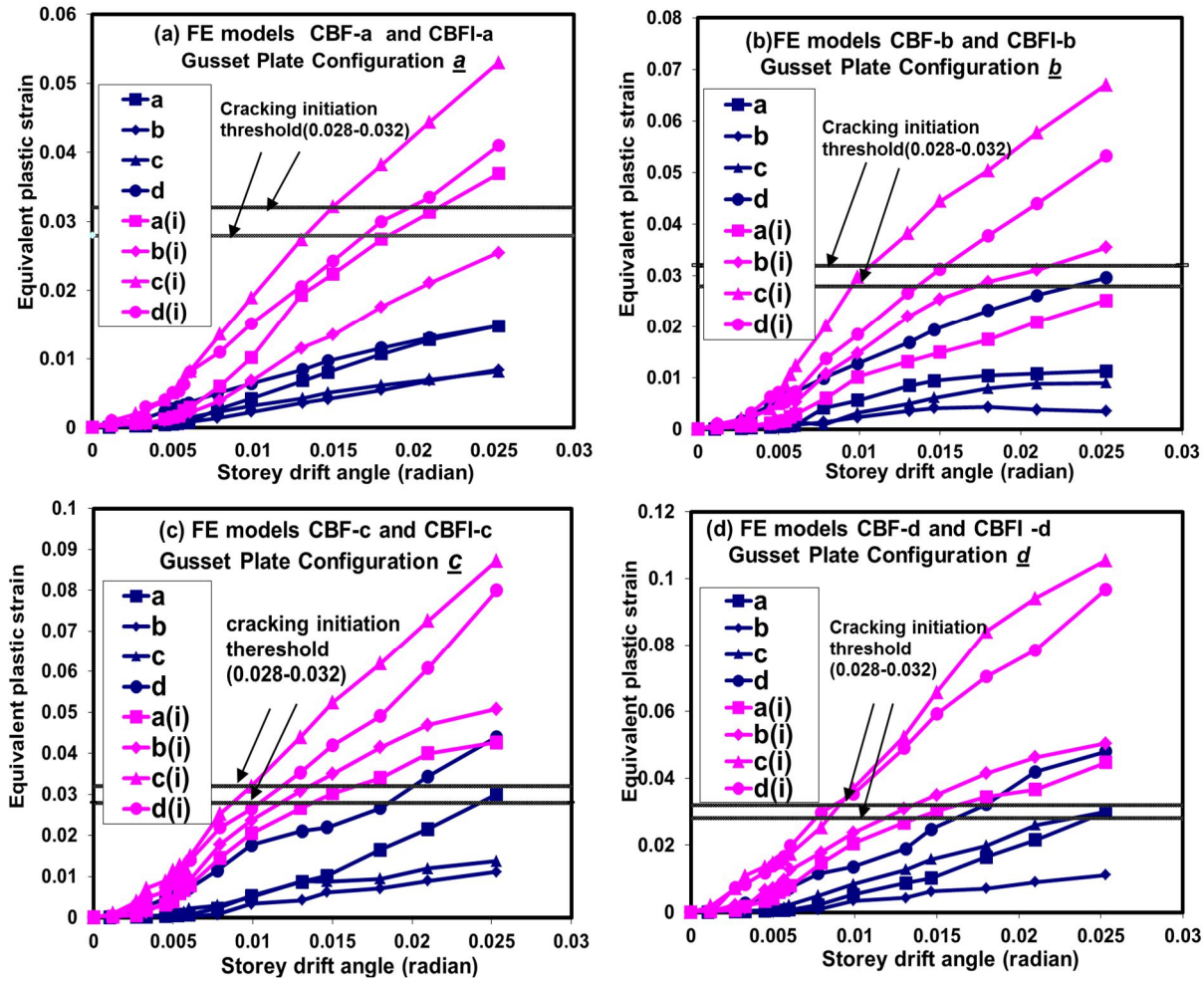

Fig. 11: Equivalent plastic strain (ε_{eqv}^{pl}) versus storey drift angle at the critical points of the gusset plates (a) Elliptical clearance 8tp; (b) Linear clearance 2tp; (c) Tapered gusset plate with taper angle of 15 degrees; (d) Tapered gusset plate with taper angle of 25 degrees

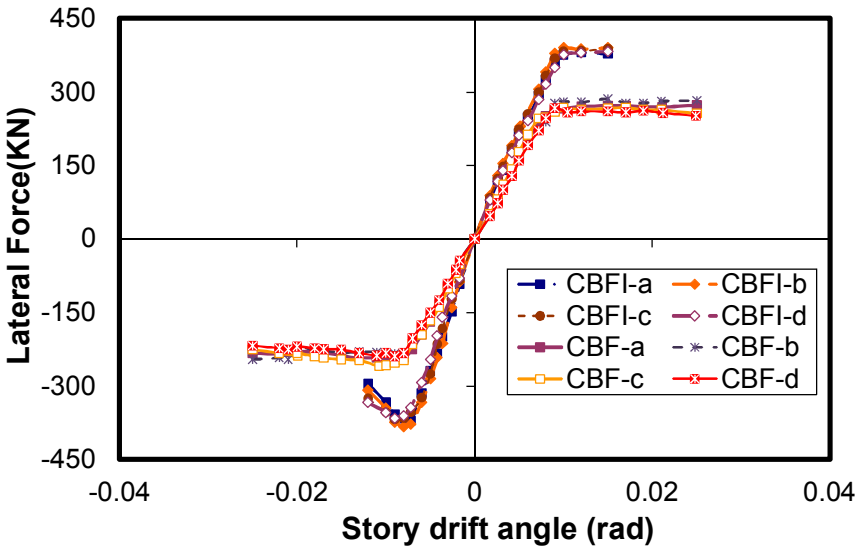

Fig. 12: Envelope of the cyclic response of CBFs using different gusset plate configurations in the presence and the absence of masonry infill

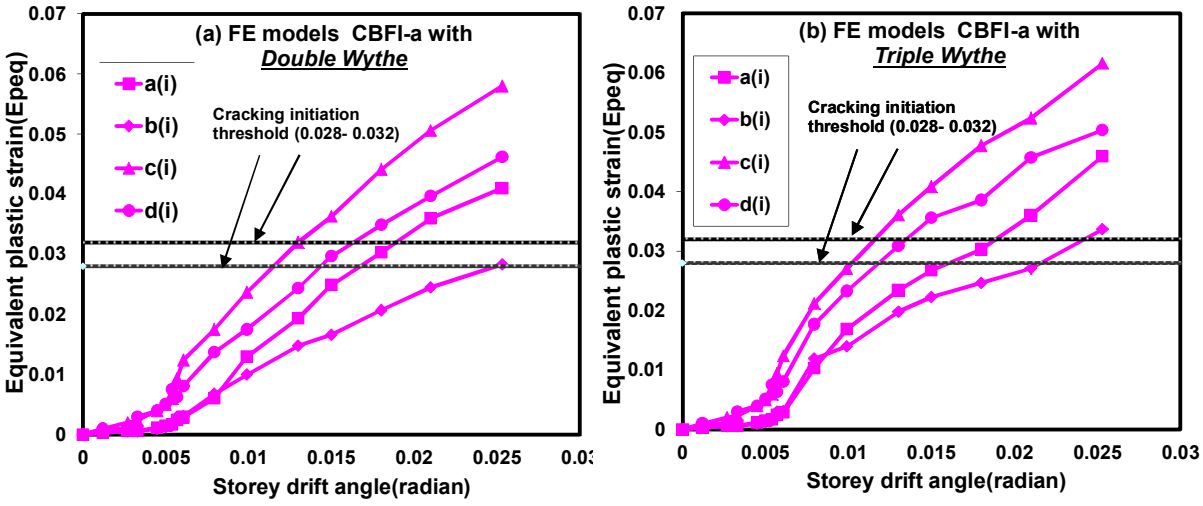

Fig. 13: Equivalent plastic strain (ε_{eqv}^{pl}) versus storey drift angle at the critical points of the gusset plates with elliptical clearance 8tp (a) double wythe; (b) triple wyrhe